Manuscript 3359

Designing of Human Serum Albumin Nanoparticles for Drug Delivery: a Potential Use of Anticancer Treatment

Ali Al-Ani

Rasha Alsahlanee

Designing of Human Serum Albumin Nanoparticles for Drug Delivery: a Potential Use of Anticancer Treatment

Abstract

Human serum albumin (HSA) nanoparticles have been widely used as versatile drug delivery systems for improving the efficiency and pharmaceutical properties of drugs. The present study aimed to design HSA nanoparticle encapsulated with the hydrophobic anticancer pyridine derivative (2-((2-([1,1'-biphenyl]-4-yl)imidazo[1,2-a]pyrimidin-3-yl)methylene)hydrazine-1-carbothioamide (BIPHC)). The synthesis of HSA-BIPHC nanoparticles was achieved using a desolvation process. Atomic force microscopy (AFM) analysis showed the average size of HSA-BIPHC nanoparticles was 80.21 nm. The percentages of entrapment efficacy, loading capacity and production yield were 98.11%, 9.77% and 91.29%, respectively. An In vitro release study revealed that HSA-BIPHC nanoparticles displayed fast dissolution at pH 7.4 compared to pH 3.4. They have also showed a higher cytotoxic activity against MCF-7 human breast cancer cells. The possible binding of the BIPHC into the tyrosine threonine kinase (TTK) was studied using molecular modeling. The findings of this study introduced a promising candidate model of HSA nanoparticles for delivering of BIPHC anticancer drug. These novel nanoparticles are characterized by their ability to carry a hydrophobic BIPHC agent and control drug release with improved targeting of breast cancer cells.

Keywords

Desolvation; Drug delivery; Glutaraldehyde; Human serum albumin; MCF-7 human breast cancer cells

RESEARCH PAPER

Designing of Human Serum Albumin Nanoparticles for Drug Delivery: A Potential Use of Anticancer Treatment

Ali Al-Ani [a,*], Rasha Alsahlanee [b]

[a] Department of Chemistry, College of Science, University of Baghdad, Baghdad, Iraq
[b] Department of Biotechnology, College of Science, University of Baghdad, Baghdad, Iraq

Abstract

Human serum albumin (HSA) nanoparticles have been widely used as versatile drug delivery systems for improving the efficiency and pharmaceutical properties of drugs. The present study aimed to design HSA nanoparticle encapsulated with the hydrophobic anticancer pyridine derivative (2-((2-([1,1′-biphenyl]-4-yl)imidazo[1,2-a]pyrimidin-3-yl) methylene)hydrazine-1-carbothioamide (BIPHC)). The synthesis of HSA-BIPHC nanoparticles was achieved using a desolvation process. Atomic force microscopy (AFM) analysis showed the average size of HSA-BIPHC nanoparticles was 80.21 nm. The percentages of entrapment efficacy, loading capacity and production yield were 98.11%, 9.77% and 91.29%, respectively. An *In vitro* release study revealed that HSA-BIPHC nanoparticles displayed fast dissolution at pH 7.4 compared to pH 3.4. They have also showed a higher cytotoxic activity against MCF-7 human breast cancer cells. The possible binding of the BIPHC into the tyrosine threonine kinase (TTK) was studied using molecular modeling. The findings of this study introduced a promising candidate model of HSA nanoparticles for delivering of BIPHC anticancer drug. These novel nanoparticles are characterized by their ability to carry a hydrophobic BIPHC agent and control drug release with improved targeting of breast cancer cells.

Keywords: Desolvation, Drug delivery, Glutaraldehyde, Human serum albumin, MCF-7 human breast cancer cells

1. Introduction

Modification of safe and inert drug delivery systems is one of the main goals of modern medicine. It is required that these systems ensure the continued release and carrying of biological active molecules to specifically target organs. Nanocarriers provide a useful tool for overcoming the obstacles linked with drug delivery [1]. Because of their high toxicity and low selectivity to cancer cells, anticancer therapies are type of drugs which require such drug delivery systems [2].

Human serum albumin (HSA) is the main protein component in human plasma [3]. It is a natural and biocompatible substance for the development of drug delivery nanoparticles. Human serum albumin nanoparticles are characterized by their tolerability when *in vivo* administered and their capacity to encapsulate a wide range of drugs in a non-specific manner. This type of nanoparticles also displays a long half-life (≈19 days), biodegradability, lack of immunogenicity and toxicity, and the excessive accumulation of HSA in tumor tissues which makes it an excellent target for drug delivery [4–6]. Biodegradable HSA is preferable, because it is fragmented into small residues that are readily removed from the body without causing any long-term side effects. Due to the increase of permeability and retention (EPR) effect, HSA macromolecules with a size lower than 200 nm can accumulate in tumor tissues [7,8]. Furthermore, albumin receptors such as the 60 kDa glycoprotein

Received 2 March 2024; revised 11 May 2024; accepted 14 May 2024.
Available online 6 June 2024

* Corresponding author.
E-mail address: ali.w@sc.uobaghdad.edu.iq (A. Al-Ani).

https://doi.org/10.33640/2405-609X.3359

(gp60) which is positioned on the surface of the endothelial cell and actively transports HSA-bound drugs, plays a role in the accumulation of drugs in tumor tissues [9]. Therefore, in recent decades, HSA was the most widely used as a versatile carrier for enhancing drug's pharmacokinetic profile and drug targeting [10,11]. Different physicochemical processes have been reported for drug encapsulation using HSA. Desolvation, emulsification, and thermal gelation are examples for such processes [10]. Among these methods, desolvation seems to be the most appropriate due to its simplicity and repeatability [12,13]. According to this technique, ethanol has been used as a desolvating agent where HSA nanoparticles are formed due to poor solubility in ethanol. Because of instability, the produced nanoparticles are rendered stable through the process of glutaraldehyde treatment. Glutaraldehyde is a cross-linking agent where its aldehyde group reacts with amine group of lysine and/or arginine residues in HSA protein. It is one of the most frequently implemented approaches that is used to prolong the half-life of HSA nanoparticles in their aqueous environment and/or inhibits the build-up of protein macro-aggregates [14,15]. Recently, several studies have modified and optimize this strategy to synthesize HSA nanoparticles for carrying different types of drug [16–18].

Imidazo [1,2-a]pyridine is a promised scaffold for synthesis of novel drug molecules in medicinal chemistry that are characterized by a wide range of biological activities [19,20]. Olprinone, Soraprazan, Zolpidem and several other compounds under preclinical assessment are some examples of commercial drugs which are reflecting wide spectrum of therapeutics in imidazo [1,2-a]pyridine scaffolds class [21]. Imidazo [1,2-a]pyridine derivatives were additionally investigated for their potential in treating certain diseases including migraines [21,22], lung cancer [23], Alzheimer's disease [24], anticancer agents [25] and viral diseases [26]. The pharmacological characteristics for these heterocyclic compounds have been extensively investigated as receptor ligands, enzyme inhibitors and anti-infectious agents [27].

Recently, 2-((2-([1,1′-biphenyl]-4-yl) imidazo [1,2-a] pyrimidin-3-yl) methylene) hydrazine-1-carbothioamide (BIPHC) compound was synthesized in our laboratory as one of Imidazo [1,2-a]pyridine derivatives [28], Fig. 1.

The aim of this study was to fabricate HSA nanoparticles by loading them with BIPHC compound for a potential use as an effective drug delivery in cancer treatment.

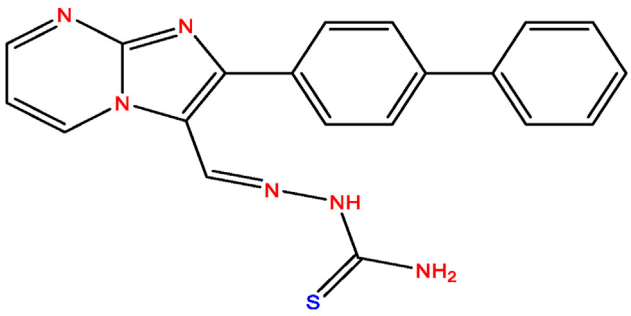

Fig. 1. The chemical structure of 2-((2-([1,1′-biphenyl]-4-yl)imidazo [1,2-a]pyrimidin-3-yl)methylene)hydrazine-1-carbothioamide.

2. Materials and methods

2.1. Materials

The human serum albumin (fraction V) with purity of 96–99%, aqueous solution of glutaraldehyde (25%), absolute ethanol, sodium hydroxide, sodium chloride, sodium dihydrogen orthophosphate, disodium hydrogen orthophosphate, RPMI medium, fetal bovine serum and 3-(4,5-dimethylthiazol-2-yl)-2,5-diphenyl tetrazolium bromide (MTT) were purchased from Sigma Aldrich.

2.2. Nanoparticles synthesis using human serum albumin

Drug-free HSA nanoparticles and BIPHC-loaded nanoparticles were crosslinked using glutaraldehyde by applying a pH-coacervation technique [29–31], Fig. 2. Briefly, HSA (100 mg) was dissolved in 2 mL of 10 mM NaCl and the pH of solution was titrated to 8 using 1 M NaOH. The BIPHC was dissolved in ethanol and incubated 5 h at room temperature. Nanoparticles were obtained by the addition of 8 mL of BIPHC in ethanol solution to HSA solution, at concentration of 5 mg BIPHC per 1 mL HSA solution, dispensed continuously at a consistent rate of 1 mL/min while being stirred magnetically. Stabilizing of formed nanoparticles was achieved by combining them with 120 μL of an 8% glutaraldehyde solution. The cross-linking was proceeding under stirring for 24 h at room temperature.

2.3. Encapsulation efficiency of BIPHC-loaded HSA nanoparticles

BIPHC-loaded HSA nanoparticles were purified using of three cycles of ultra-centrifugation (20,000×*g*, 30 min). The pellets re-dissolved in NaCl solution to original volume. Following the purification process, the estimation of entrapment efficacy

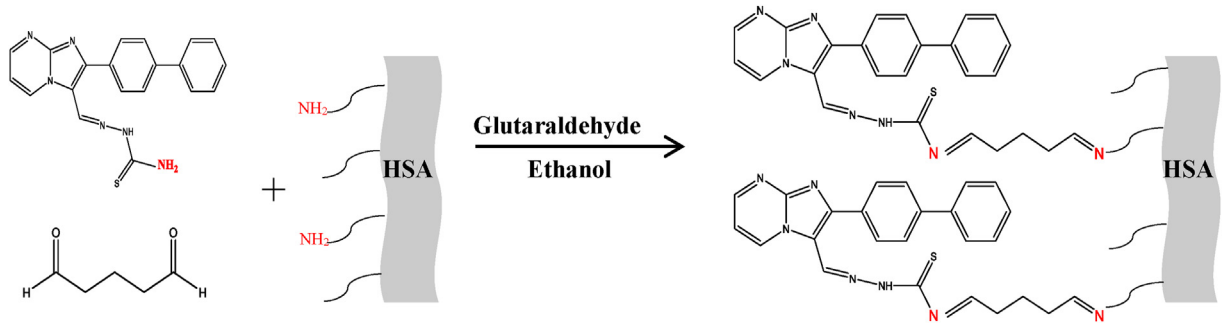

Fig. 2. Proposed reaction between HSA and BIPHC in the presence of glutaraldehyde as crosslinking agent.

percentage, loading capacity and production yield were carried out using the measurement of unloaded free BIPHC present in the supernatant using spectrophotometer.

Entrapment efficacy (%) = (Total amount of drug - Free drug) / (Total amount of drug) X100

Loading capacity (%) = (Total amount of drug - Free drug) / (Total weight of nanoparticles) X100

Production yield (%) = (Total amount of nanoparticles) / (Total weight of BIPHC and HSA) X100

2.4. Physico-chemical characterization of HSA-BIPHC nanoparticles

Size, morphology, surface texture and roughness of the formed nanoparticles were analyzed using atomic force microscopy (AFM). In brief, the sample for AFM was prepared by placing a well-dispersed droplet of nanoparticle on a microscope slide. Then the sample was air dried at room temperature overnight to remove of moisture and applied for AFM analysis (SPM AA3000, Angstrom Advanced Inc., USA).

Absorption and emission of nanoparticles were also determined using (UV-1800 UV−Vis spectrophotometer, Shimadzu, Japan) and (Shimadzu rf-5301 spectrofluorophotometer), respectively.

2.5. Study of drug release

The dialysis approach was used to conduct an *in vitro* release profile of BIPHC from HSA nanoparticles. A dialysis tube (molecular weight cut-off: 8 kDa) containing HSA-BIPHC nanoparticles (1 mL) was soaked in 100 mL phosphate buffer saline (PBS) (pH 7.4 or pH 3.4) and continuously stirred on a shaker over 10 days. At selected time intervals, 1 mL of the medium was withdrawn for measurement of released BIPHC and the medium was replenished with freshly prepared PBS.

2.6. In vitro assessment of HSA-BIPHC cytotoxicity

For this investigation, human breast cancer epithelial cells (MCF-7) were chosen. Under optimal conditions, these cells were cultured in RPMI medium that was supplemented with 10% (v/v) fetal bovine serum and subcultured twice weekly to maintain logarithmic growth.

The cell viability was evaluated using MTT assay. Into 96-well plates, cells were seeded at a density of nearly 3×10^3 cells/well and incubated at 37 °C for 24 h in a 5% CO_2 environment to allow the cells to adhere on the plates. For 72 h at 37 °C, these cells were exposed to HSA-BIPHC at final concentrations 10, 20, 40, and 80 μg/mL in order to facilitate the agent's absorption. The excess of HSA-BIPHC agent containing medium was removed by aspiration and then twice rinsed with 200 μL of RPMI medium. Next, 200 μL of RPMI medium and 50 μL of MTT (2 mg/mL) were added to each well and incubated for 3 h at 37 °C in a 5% CO_2. Each well had 150 μL DMSO used to dissolve formazan crystals after the medium was aspirated. The absorbance was recorded at 550 nm, via a microplate reader (En Vision 2104, PerkinElmer).

2.7. Docking study

In this study, Chem. Draw was used to draw, energy minimization and set charges of the BIHPC ligand and then converted to Auto Dock ligand (pdbqt). The crystal structure of the human tyrosine threonine kinase (TTK) receptor was retrieved from

the protein Data Bank (PDB ID:6N6O). The interaction between BIHPC and TTK was analyzed using Auto dock 1.5.7 [32]. All docking processes for the possible binding modes between the ligands and the target were performed using default settings.

3. Results and discussion

3.1. Preparation of HSA-BIPHC

Human serum albumin nanoparticles have been widely used as versatile drug delivery systems for improving the efficiency and pharmaceutical properties of drugs [33,34]. In this study, BIPHC was coated with HSA for fabrication of new drug delivery system. The BIPHC compound was synthesized previously in our laboratory [28]. This substance is a derivative of Imidazo [1,2-a]pyridine, which serve as the scaffold for synthetic of novel drug molecules with a wide range of biological activities [19]. Desolvation method was used for synthesis of HSA-BIPHC particles in nano-size. In this method ethanol was employed as a desolvating agent where HSA nanoparticles were generated as a result of their restricted solubility in ethanol. Glutaraldehyde was also used for stabilizing the formed nanoparticles through cross-linking between BIPHC and HSA.

3.2. Characterization of HSA-BIPHC

The HSA-BIPHC nanoparticles demonstrated an entrapment efficacy of 98.11%, a loading capacity of 9.77% and production yield of 91.29%. These results indicate that the encapsulation was efficiently proceeded to form HSA-BIPHC nanoparticles.

The formed HSA-BIPHC nanoparticle was analyzed using AFM technique. The AFM technique was used to confirm the formation of HSA-BIPHC in nano-size as well as to study the morphology, surface texture and roughness of the formed nanoparticles, Table 1 and Fig. 3. AFM images show that the average diameter of HSA-BIPHC nanoparticles was clearly reduced in comparison to the average diameter of HSA and BIPHC particles. Nanoparticles formed by the desolvation method have an average diameter of 80.21 nm and having an even surface. This size of nanoparticles may primarily be eliminated through bile and faeces, according to pharmacokinetic research conducted by Abraxane® [35,36]. According to several studies, the size of HSA-BIPHC nanoparticle is perfect for drug accumulation in the extravascular space of tumors via EPR effect [7,8,33].

Table 1. Particle size distribution of HSA-BIPHC nanoparticles.

Diameter (nm)	HSA	BIPHC	HSA- BIPHC
Avg. Diameter	110.26	82.01	80.21
≤10% Diameter	0	0	55.00
≤50% Diameter	100.00	75.00	75.00
≤90% Diameter	140.00	105.00	110.00

Fig. 4 shows the maximum excitation and emission spectra of HSA-BIPHC nanoparticles occur at 420 nm and 485 nm, respectively. The dye of BIPHC enables to use this compound as a fluorescent probe for *in vivo* and *in vitro* biomedical studies. Our results indicate that there was no overlapping in the maximum excitation and emission spectrum of HSA-BIPHC nanoparticles. However, there was an overlapping in other excitation and emission peaks above the maximum emission wavelength. It is well known that most organic fluorophore molecules have a lower resolution due to the overlapping in there emission spectra, the defects that hindered the using of these fluorophore agent in biological systems imaging [37]. As there was no overlapping between the maximum excitation and emission spectra, this result gives an advantage to use HSA-BIPHC nanoparticles as a probe for the imaging of the targeting cells as well as follow the accumulation of these nanoparticles in tumor tissues using fluorescence microscope. Furthermore, excitation and emission wavelengths for these nanoparticles are far from the hazardous UV region (240 nm–300 nm) and are safe to use for the bioanalysis and bioanalytical trials [37].

3.3. Drug release mechanism

Fig. 5 shows *in vitro* release of the BIPHC from nanoparticles under physiological pH (pH 7.4) and under the pH of stomach (pH 3.4). The primary goal of controlling the release of drug into the bloodstream is to maintain a drug concentration between the therapeutic window, which is defined as the range between minimum toxic concentration (MTC) and the minimum effective concentration (MEC) [38,39]. The administration of drug in a single large dose leads to the drug elevated in the level higher than MTC, producing toxic side effects, and then quickly drops down to the MEC. Therefore, it is required to modify drug carriers that controlled drug release in a frequency with low dosage. The mechanism by which BIPHC released from nanoparticles is known degradation-controlled release. Degradation-controlled release includes releasing of drugs from biodegradable polymers via enzymatic and/or hydrolytic degradation of the bonds in their backbones. The BIPHC release kinetics can be described in three phases, showing an initial slow

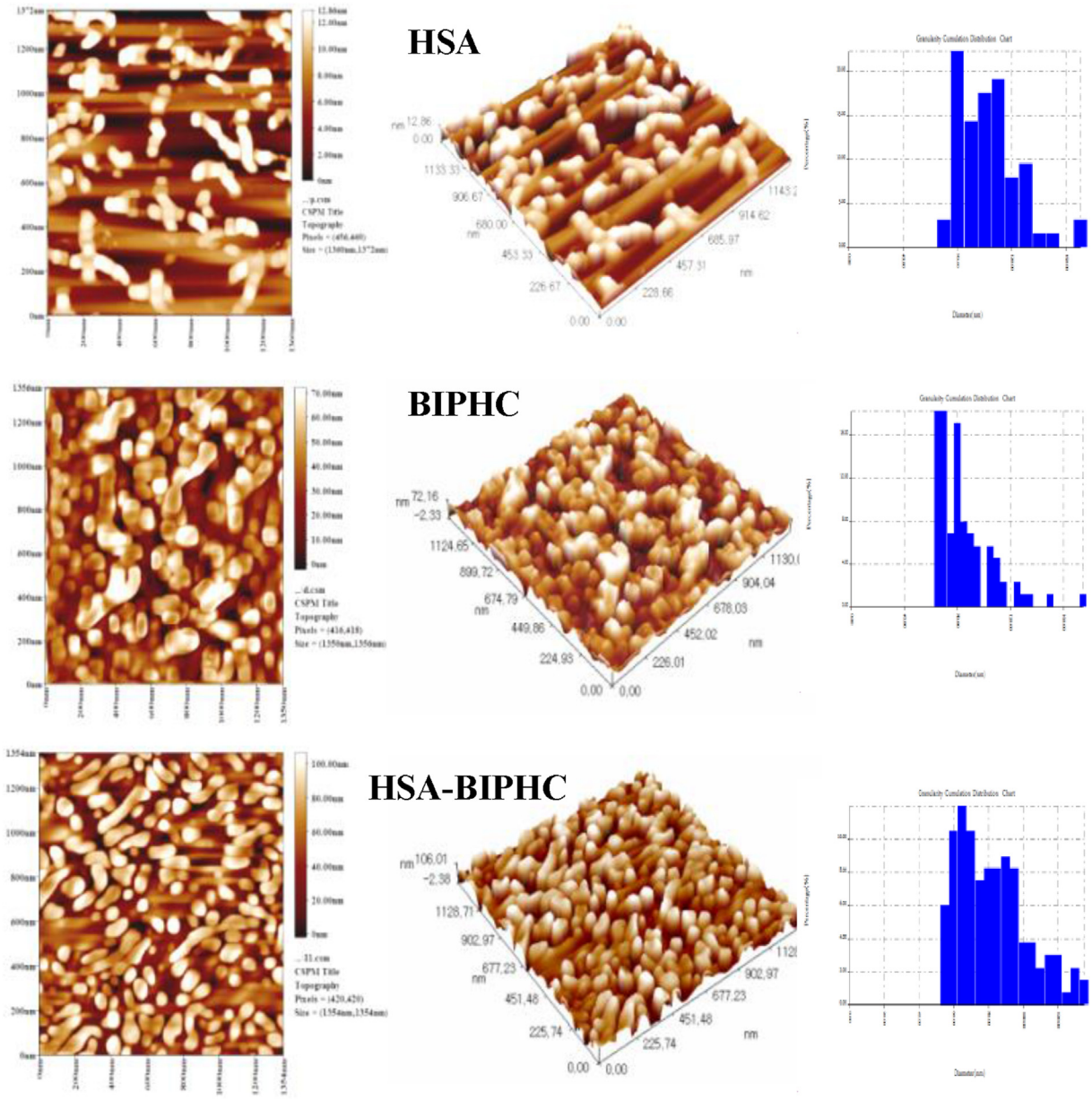

Fig. 3. AFM images for HSA-BIPHC nanoparticles, the first column presents a 2D image, the second column displays a 3D image and the third column represents the size granulated distribution for HSA-BIPHC.

release during the first 96 h at pH 7.4 and 120 h at pH 3.4, subsequently, the second phase ensues, characterized by a rapid release, and ultimately, the third stage, involving a gradual and controlled release of the remaining BIPHC.

During the time of rapid release, about 95% of BIPHC was released. The most suitable model for the BIPHC release data is the diffusion-controlled release rate, in which the rate that the drug molecules are released decreases over time as a result of decreases in the concentration gradient. Furthermore, a difference in the release rate can be explained by a difference in the response of BIPHC and HSA to the pH of buffer solution.

Our finding is consistent with study by A. Al-Ani *et al*. (2021) which carried on gelatin-polyethylene glycol nanoparticles and a study by M. Rajan *et al*. (2012) which includes preparation of the rifampicin–chitosan– polyethylene glycol nanoparticles. Both studies indicated that electrostatic interactions of synthesized nanoparticles were easily hydrolyzed at physiological pH compared to acidic pH [40,41]. In contrast, hyaluronic acid–chitosan–lipoic acid nanoparticle which was

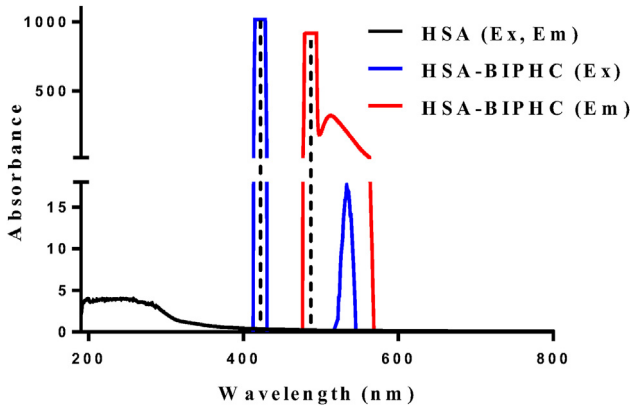

Fig. 4. Excitation and emission spectra of HSA-BIPHC nanoparticles.

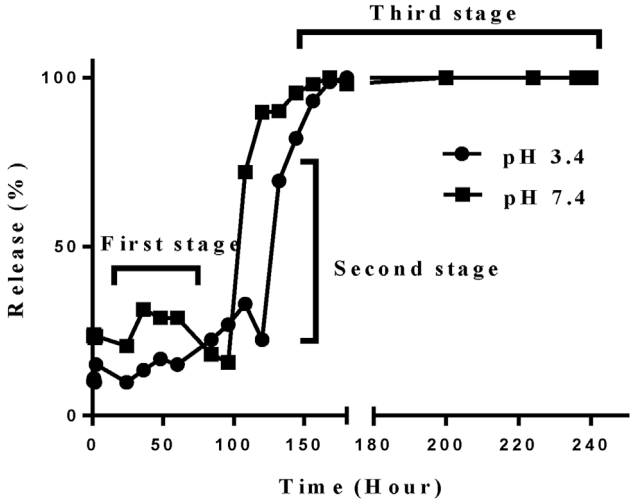

Fig. 5. Drug release graph shows a cumulative release (%) of BIPHC from HSA.

designed by S. Rezaei *et al*. (2020) showed a reduce in releasing of 17 −Methyltestosterone at pH 7.4 compared to pH 6.5 [42].

It was also noticed that HSA-BIPHC nanoparticles can be controlled the BIPHC release rate from the carrier which might be contributed to improving therapeutic efficacy and reducing toxicity of a BIPHC.

3.4. In vitro *study of cell viability*

The suppressive growth effects of HSA-BIPHC and BIPHC on MCF-7 cancer cell line derived from human breast were studied by employing the 3-(4,5-dimethylthiazol-2-yl)-2,5-diphenyltetrazolium bromide (MTT) assay, Fig. 6. Breast cancer is the most common diagnosed life-threatening cancer leading cause of oncologic mortality and morbidity in women worldwide [43]. Recent breast cancer

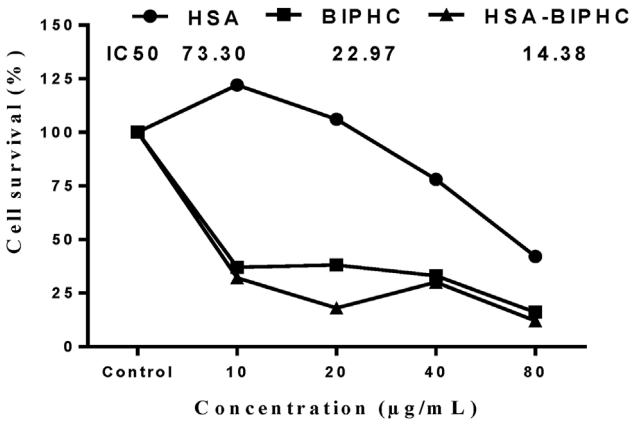

Fig. 6. MTT assay on MCF-7 cells treated with HSA, BIPHC and HSA-BIPHC after 72 h incubation at 37 °C and 5% of CO_2.

treatment options consist of several medications that have limited effectiveness; however, there is a need for new and innovative therapeutic approaches, particularly for breast cancers that metastatic and drug-resistant breast cancers [44]. After been exposed for 72 h, the growth of MCF-7 cells was inhibited in a dose-dependent manner when HSA-BIPHC was present. The IC50 value, which represents the concentration at which 50% growth inhibition occur, was found to be 14.38 µg mL^{-1}. This value is much lower than the IC50 value reported for HSA alone (73.30 µg mL^{-1}) and BIPHC alone (22.97 µg mL^{-1}), as shown in Fig. 6. These results suggest that the HSA-BIPHC was recognized by MCF-7 cells. The coating with HSA leads to selectively enhance the uptake of BIPHC as nanoparticles which induce cytotoxic effects on MCF-7 cancerous cells. Albumin receptors, such as the 60 kDa glycoprotein (gp60) positioned on the surface of endothelial cell, which actively transport of HSA-bound drugs, play a role in the accumulation of drugs in tumor tissues [9].

3.5. Docking study

The *in vitro* results encourage performing molecular docking studies to screen the BIPHC compound, inculcating both *in vitro* and *in silico* results. Threonine Tyrosine kinase (TTK) is a crucial component that controls the development of cells through mitosis by regulating of the spindle assembly checkpoint (SAC). It is a surveillance mechanism that guarantees the chromosome fidelity segregation. Cellular mechanism confirms that inhibition of TTK activity leads to increase cell death by apoptosis through accumulation of chromosome segregation errors which accelerate mitotic exit [45]. The TTK was discovered through screening of *in*

vivo phenotypic of a triple-negative breast cancer (TNBC) cell line [46]. Recently, TTK has been reported as a promising therapeutic target for TNBC and other human cancers [47]. Therefore, the molecular docking was conducted on the crystal structure of TTK considering it as the target receptor using AutoDock 1.5.7. The RMSD, binding energy, inhibition constant (Ki), number of H-bonds (drug-Enzyme) and amino acids involved in interaction were calculated to predict orientation, binding modes and affinities of BIPHC, Fig. 7. The TTK comprising couples lobed kinase structure with 857

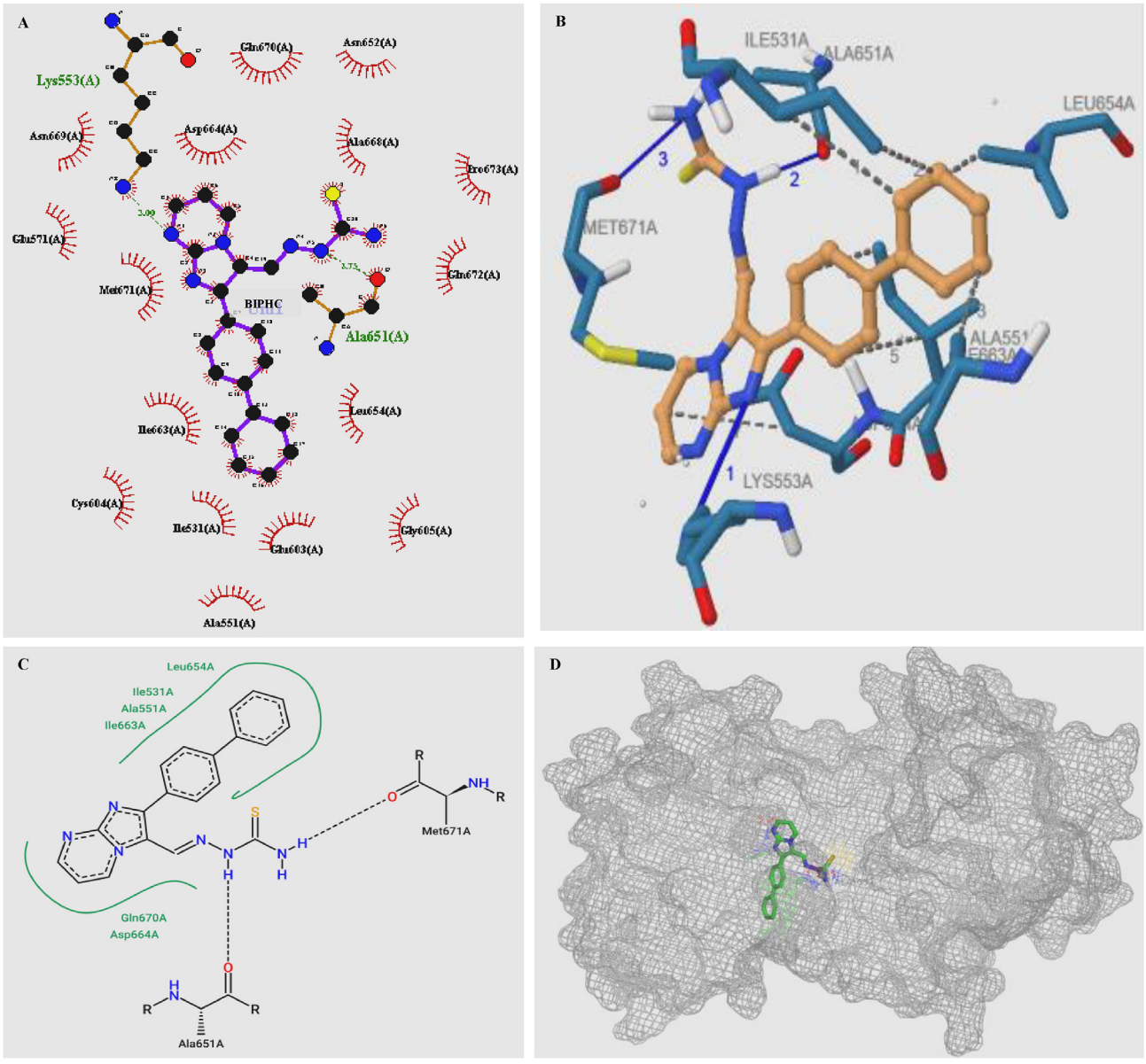

Protein	Compound	RMSD	Binding energy (Kcal/Mol)	Inhibition constant (Ki, nM)	No. of H bonds (drug-Enzyme)	Amino acids involved in interaction
TTK	BIPHC	40.66	-9.15	197.37	3	531ILE, 551ALA, 654LEU, 663ILE, 664ASP, 553LYS, 651ALA, 671MET

Fig. 7. Docking pose of the BIPHC compound at the TTK crystal structure. (A) The ligplot results for TKK, showing all amino acid residues of active pocket and, (B) the PLIP result shows the H-bonds formation, (C) the proteins plus result shows the localized of BIPHC in the active pocket and (D) the Pymol image shows the best and stable conformations of the synthesized BIPHC.

amino acids. It includes C-terminal activation and catalytic loop having residues ranging from (Asn606-Gln794), the N-terminal lobe (Glu516-Met602), six beta sheets and one alpha helix. Both lobes link the hinge region through Glu603 and Gly605 residues [47]. Kinase proteins catalyze the transfer of the γ-phosphate from ATP to the receiver substrate. Several inhibitor templates were discovered to design drugs that can target the ATP binding site of various members of the kinase family [48]. The docking of TTK receptor with BIPHC candidate ligand exhibited well established bonds with receptor active pocket of one or more amino acids. Our study revealed that the synthesized BIPHC showed a good binding energy toward the target TTK protein (-9.15 kcal mol^{-1}). A crystal structure of the kinase domain of TTK revealed a formation of H-bond between the N-6 of Imidazo [1,2-a]pyrimidin and the side chain of Lys553 residue and blocks the contact between Lys553 and Glu571 of Helix C and prevents binding of ATP, Fig. 7A and B.

According to the finding, the kinase becomes inactive because the salt bridge between the conserved lysine and glutamate residues was destroyed, which prevents it from efficiently processing substrates [48]. Fig. 7A also shows that BIPHC was positioned close proximity to the gatekeeping of Cys604 and Gly605 hinge residues, the ATP-binding site which is crucial for effectively inhibiting protein kinases. Fig. 7C shows that BIPHC was localized in a pocket lined by Ile663, Leu654 and by Gln670, Asp 664 the residues of C-terminal activation and catalytic loop. This position allows the BIPHC to block the activation and catalytic site of TTK with the best and stable conformations of the synthesized BIPHC, Fig. 7D. A strong positive correlation ($R = 0.99$ and $p < 0.0001$) was observed between the binding energy and the Ln of inhibition constant (Ki). This indicates that with more binding energy toward TTK, the BIPHC has a higher inhibitor activity, Fig. 8.

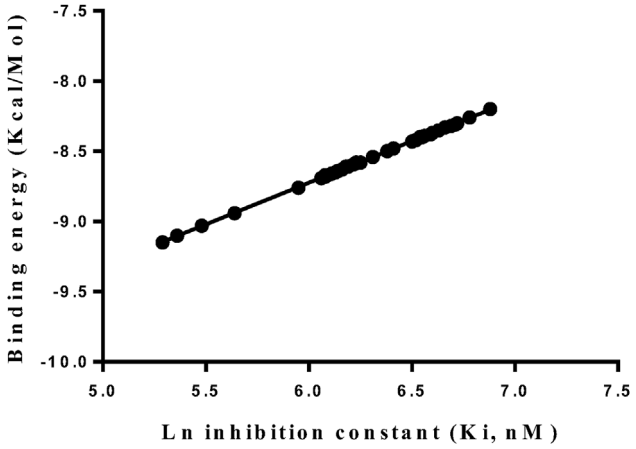

Fig. 8. Pearson correlation between binding energy of 45 favorable binding poses and the Ln of inhibition constant.

Finally, this study was successful in presenting novel HSA-BIPHC nanoparticles that are characterized by their ability to carry a hydrophobic BIPHC and control it's released with improved targeting to breast cancer cells.

4. Conclusion

Novel HSA-BIPHC nanoparticles were successfully prepared with an average diameter of 80.21 nm and smooth surface. HSA-BIPHC nanoparticles can control the BIPHC release rate from the carrier which might contribute in improving therapeutic efficacy and reducing the toxicity of a BIPHC. Encapsulation with HSA leads to selectively enhancing the uptake of BIPHC as nanoparticles and inducing cytotoxic effects in MCF-7 cancerous cells. *In silico*, results show that BIPHC compound could fit in the active site of the TTK and thus BIPHC can be used as an inhibitor for TTK in cancer cells. It can be concluded that using HSA-BIPHC nanoparticles as a drug delivery system, not only enhance tumor-targeting drug delivery but also control the BIPHC release rate, improving therapeutic efficacy and reducing the toxicity of BIPHC. However, many issues need to be studied for translating new HSA-BIPHC nanoparticles to clinically active products. One of the subjects the behaviour of these nanoparticles *in vivo*.

Funding

We didn't receive any funding or grant from any source. It is completely self-support.

Ethics information

All research reported in submitted papers has been conducted in an ethical and responsible manner. Also this study didn't involving humans, animals, plants, biological material, protected or non-public datasets.

Conflicts of interest

The authors report there are no competing interests to declare.

Acknowledgements

The authors would like to thank the technicians of the Chemistry Department and Biotechnology

Department in the University of Baghdad for their help in conducting measurements.

References

[1] M. Pourmadadi, S. Ostovar, G. Ruiz-Pulido, D. Hassan, M. Souri, A.-L.E. Manicum, R. Behzadmehr, S. Fathi-karkan, A. Rahdar, D.I. Medina, Novel epirubicin-loaded nano-formulations: advancements in polymeric nanocarriers for efficient targeted cellular and subcellular anticancer drug delivery, Inorg Chem Commun 155 (2023) 110999, https://doi.org/10.1016/j.inoche.2023.110999.

[2] S. Adepu, S. Ramakrishna, Controlled drug delivery systems: current status and future directions, Molecules 26 (2021) 5905, https://doi.org/10.3390/molecules26195905.

[3] Y. Wang, H. Li, J. Lan, R. Guan, Y. Bao, X. Du, Z. Zhao, R. Shi, H. Hollert, X. Zhao, The weakened physiological functions of human serum albumin in presence of polystyrene nano-plastics, Int J Biol Macromol 261 (2024) 129609, https://doi.org/10.1016/j.ijbiomac.2024.129609.

[4] J. Wasko, M. Wolszczak, Z. Zajaczkowska, M. Dudek, B. Kolesinska, Human serum albumin as a potential drug delivery system for N-methylated hot spot insulin analogs inhibiting hormone aggregation, Bioorg Chem 143 (2024) 107104, https://doi.org/10.1016/j.bioorg.2024.107104.

[5] I.L. de Redín, C. Boiero, M.C. Martínez-Ohárriz, M. Agüeros, R. Ramos, I. Peñuelas, D. Allemandi, J.M. Llabot, J.M. Irache, Human serum albumin nanoparticles for ocular delivery of bevacizumab, Int J Pharm 541 (2018) 214–223, https://doi.org/10.1016/j.ijpharm.2018.02.003.

[6] S. Sharma, R. Parveen, B.P. Chatterji, Toxicology of nano-particles in drug delivery, Curr Pathobiol Rep 9 (2021) 133–144, https://doi.org/10.1007/s40139-021-00227-z.

[7] L. Yu, Z. Hua, X. Luo, T. Zhao, Y. Liu, Systematic interaction of plasma albumin with the efficacy of chemotherapeutic drugs, Biochim Biophys Acta Rev Cancer 1877 (2022) 188655, https://doi.org/10.1016/j.bbcan.2021.188655.

[8] C.R. Park, M.G. Song, J.-Y. Park, H. Youn, J.-K. Chung, J.M. Jeong, Y.-S. Lee, G.J. Cheon, K.W. Kang, Conjugation of arginylglycylaspartic acid to human serum albumin decreases the tumor-targeting effect of albumin by hindering its secreted protein acidic and rich in cysteine-mediated accumulation in tumors, Am J Transl Res 12 (2020) 2488–2498.

[9] K. Kimura, K. Yamasaki, K. Nishi, K. Taguchi, M. Otagiri, Investigation of anti-tumor effect of doxorubicin-loaded human serum albumin nanoparticles prepared by a desolvation technique, Cancer Chemother Pharmacol 83 (2019) 1113–1120, https://doi.org/10.1007/s00280-019-03832-3.

[10] A.S. Chubarov, Serum albumin for magnetic nanoparticles coating, Magnetochemistry 8 (2022) 13, https://doi.org/10.3390/magnetochemistry8020013.

[11] C. Li, D. Zhang, Y. Pan, B. Chen, Human serum albumin based nanodrug delivery systems: recent advances and future perspective, Polymers 15 (2023) 3354, https://doi.org/10.3390/polym15163354.

[12] O. Esim, C. Hascicek, Albumin-based nanoparticles as promising drug delivery systems for cancer treatment, Curr Pharmaceut Anal 17 (2021) 346–359, https://doi.org/10.2174/1573412916999200421142008.

[13] R. Meng, H. Zhu, Z. Wang, S. Hao, B. Wang, Preparation of drug-loaded albumin nanoparticles and its application in cancer therapy, J Nanomater 2022 (2022) 1–12, https://doi.org/10.1155/2022/3052175.

[14] K. Kimura, K. Yamasaki, H. Nakamura, M. Haratake, K. Taguchi, M. Otagiri, Preparation and in vitro analysis of human serum albumin nanoparticles loaded with anthracycline derivatives, Chem Pharm Bull (Tokyo) 66 (2018) 382–390, https://doi.org/10.1248/cpb.c17-00838.

[15] J. Jayanudin, R.S. Lestari, I. Kustiningsih, D. Irawanto, R. Rozak, R.L. Wardana, F. Muhammad, Sustainable material for urea delivery based on chitosan cross-linked by glutaraldehyde saturated toluene: characterization and determination of the release rate mathematical model, Karbala Int J Mod Sci. 8 (2022) 657–669, https://doi.org/10.33640/2405-609X.3266.

[16] K. Patel, P. Jain, P.K. Rajput, A.K. Jangid, R. Solanki, H. Kulhari, S. Patel, Human serum albumin-based propulsive Piperlongumine-loaded nanoparticles: formulation development, characterization and anti-cancer study, Colloids Surf A Physicochem Eng Asp 652 (2022) 129738, https://doi.org/10.1016/j.colsurfa.2022.129738.

[17] P. Ghosh, S. Bag, P. Roy, P.I. Chakraborty, S. Dasgupta, Permeation of flavonoid loaded human serum albumin nanoparticles across model membrane bilayers, Int J Biol Macromol 222 (2022) 385–394, https://doi.org/10.1016/j.ijbiomac.2022.09.186.

[18] S. Zaher, M.E. Soliman, M. Elsabahy, R.M. Hathout, Sesamol loaded albumin nanoparticles: a boosted protective property in animal models of oxidative stress, Pharmaceuticals 15 (2022) 733, https://doi.org/10.3390/ph15060733.

[19] M. Sharma, P. Prasher, C2-functionalized imidazo [1, 2-a] pyridine: synthesis and medicinal relevance, Synth Commun 52 (2022) 1337–1356, https://doi.org/10.1080/00397911.2022.2079091.

[20] A.H. Hamd, N. Al-Lami, Anti-breast cancer activity of some synthesized pyrazole derivatives bearing imidazo [1, 2a] pyridine moiety, Iraqi J Sci 64 (2023) 3205–3217, https://doi.org/10.24996/ijs.2023.64.7.1.

[21] N. Devi, D. Singh, R. K Rawal, J. Bariwal, V. Singh, Medicinal attributes of imidazo [1, 2-a] pyridine derivatives: an update, Curr Top Med Chem 16 (2016) 2963–2994, https://doi.org/10.2174/1568026616666160506145539.

[22] N.C. Desai, J.D. Monapara, A.M. Jethawa, U. Pandit, Contemporary development in the synthesis and biological applications of pyridine-based heterocyclic motifs, in: P. Singh, eds., Recent Developments in the Synthesis and Applications of Pyridines, Elsevier. 2023, pp. 253–298, https://doi.org/10.1016/B978-0-323-91221-1.00007-5.

[23] K. Bhavya, M. Mantipally, S. Roy, L. Arora, V.N. Badavath, M. Gangireddy, S. Dasgupta, R. Gundla, D. Pal, Novel imidazo [1, 2-a] pyridine derivatives induce apoptosis and cell cycle arrest in non-small cell lung cancer by activating NADPH oxidase mediated oxidative stress, Life Sci 294 (2022) 120334, https://doi.org/10.1016/j.lfs.2022.120334.

[24] P. Mishra, S. Basak, A. Mukherjee, B. Ghosh, Pyridines in Alzheimer's disease therapy: recent trends and advancements, in: P. Singh, eds., Recent Developments in the Synthesis and Applications of Pyridines, Elsevier. 2023, pp. 159–188, https://doi.org/10.1016/B978-0-323-91221-1.00001-4.

[25] S. Annareddygari, V. Kasireddy, J. Reddy, Synthesis of novel amide-functionalized imidazo [1, 2-a] pyrimidin-5 (1H)-ones and their biological evaluation as anticancer agents, Russ J Org Chem 58 (2022) 412–418, https://doi.org/10.1134/S1070428022030216.

[26] A. Gueiffier, S. Mavel, M. Lhassani, A. Elhakmaoui, R. Snoeck, G. Andrei, O. Chavignon, J.-C. Teulade, M. Witvrouw, J. Balzarini, Synthesis of imidazo [1, 2-a] pyridines as antiviral agents, J Med Chem Sci 41 (1998) 5108–5112, https://doi.org/10.1021/jm981051y.

[27] C. Enguehard-Gueiffier, A. Gueiffier, Recent progress in the pharmacology of imidazo [1, 2-a] pyridines, Mini Rev Med Chem 7 (2007) 888–899, https://doi.org/10.2174/138955707781662645.

[28] T. A Rehan, N. Lami, N.A. Khudhair, Synthesis, characterization and anti-corrosion activity of new triazole, thiadiazole and thiazole derivatives containing imidazo [1, 2-a] pyrimidine moiety, Chem Methodol 5 (2020) 285–295, https://doi.org/10.22034/chemm.2021.130448.

[29] C. Weber, J. Kreuter, K. Langer, Desolvation process and surface characteristics of HSA-nanoparticles, Int J Pharm 196 (2000) 197–200, https://doi.org/10.1016/S0378-5173(99)00420-2.

[30] W. Lin, A. Coombes, M. Davies, S. Davis, L. Illum, Preparation of sub-100 nm human serum albumin nanospheres using a pH-coacervation method, J Drug Target 1 (1993) 237–243, https://doi.org/10.1021/jm981051y.
[31] S. Sebak, M. Mirzaei, M. Malhotra, A. Kulamarva, S. Prakash, Human serum albumin nanoparticles as an efficient noscapine drug delivery system for potential use in breast cancer: preparation and in vitro analysis, Int J Nanomed 5 (2010) 525, https://doi.org/10.2147/IJN.S10443.
[32] M.F. Sanner, Python: a programming language for software integration and development, J Mol Graph Model 17 (1999) 57–61.
[33] B. Zhang, S. Wan, X. Peng, M. Zhao, S. Li, Y. Pu, B. He, Human serum albumin-based doxorubicin prodrug nanoparticles with tumor pH-responsive aggregation-enhanced retention and reduced cardiotoxicity, J Mater Chem B 8 (2020) 3939–3948, https://doi.org/10.1039/D0TB00327A.
[34] E. Ertugen, A. Tunçel, F. Yurt, Docetaxel loaded human serum albumin nanoparticles; synthesis, characterization, and potential of nuclear imaging of prostate cancer, J Drug Deliv Sci Technol 55 (2020) 101410, https://doi.org/10.1016/j.jddst.2019.101410.
[35] V.P. Chauhan, T. Stylianopoulos, J.D. Martin, Z. Popović, O. Chen, W.S. Kamoun, M.G. Bawendi, D. Fukumura, R.K. Jain, Normalization of tumour blood vessels improves the delivery of nanomedicines in a size-dependent manner, Nat Nanotechnol 7 (2012) 383–388, https://doi.org/10.1038/nnano.2012.45.
[36] C. Jiang, H. Cheng, A. Yuan, X. Tang, J. Wu, Y. Hu, Hydrophobic IR780 encapsulated in biodegradable human serum albumin nanoparticles for photothermal and photodynamic therapy, Acta Biomater 14 (2015) 61–69, https://doi.org/10.1016/j.actbio.2014.11.041.
[37] H. Kobayashi, M. Ogawa, R. Alford, P.L. Choyke, Y. Urano, New strategies for fluorescent probe design in medical diagnostic imaging, Chem Rev 110 (2010) 2620–2640, https://doi.org/10.1021/cr900263j.
[38] B. Mukherjee, Fundamentals of pharmacokinetics, in: B. Mukherjee, eds., Pharmacokinetics: Basics to Applications, Springer, Singapore. 2022, pp. 1–20, https://doi.org/10.1007/978-981-16-8950-5.
[39] J.H. Lee, Y. Yeo, Controlled drug release from pharmaceutical nanocarriers, Chem Eng Sci 125 (2015) 75–84, https://doi.org/10.1016/j.ces.2014.08.046.
[40] A.W. Al-Ani, J. Jeber, A. Elewi, Development of a nanostructured double-layer coated tablet based on polyethylene glycol/gelatin as a platform for hydrophobic molecules delivery, Egypt J Chem 64 (2021) 1759–1767, https://doi.org/10.21608/ejchem.2021.52019.3066.
[41] M. Rajan, V. Raj, Encapsulation, characterisation and in-vitro release of anti-tuberculosis drug using chitosan-poly ethylene glycol nanoparticles, Int J Pharm Pharmaceut Sci 4 (2012) 255–259, https://doi.org/10.1016/j.ijpharm.2013.06.030.
[42] S. Rezaei, S. Kashanian, Y. Bahrami, L.J. Cruz, M. Motiei, Redox-sensitive and hyaluronic acid-functionalized nanoparticles for improving breast cancer treatment by cytoplasmic 17α-methyltestosterone delivery, Molecules 25 (2020) 1181, https://doi.org/10.3390/molecules25051181.
[43] N.M. Abd Al-Hameed, A.W. Al-Ani, The role of monoamine oxidase and atherogenic index in newly diagnosed and tamoxifen treated women with breast cancer, J Med Chem Sci. 6 (2023) 645–655, https://doi.org/10.26655/JMCHEMSCI.2023.3.21.
[44] A.W. Al-Ani, F. Zamberlan, L. Ferreira, T.D. Bradshaw, N.R. Thomas, L. Turyanska, Near-infrared PbS quantum dots functionalized with affibodies and ZnPP for targeted imaging and therapeutic applications, Nano Express 2 (2021) 040005, https://doi.org/10.1088/2632-959X/ac33b8.
[45] J.C. Uitdehaag, J. de Man, N. Willemsen-Seegers, M.B. Prinsen, M.A. Libouban, J.G. Sterrenburg, J.J. de Wit, J.R. de Vetter, J.A. de Roos, R.C. Buijsman, Target residence time-guided optimization on TTK kinase results in inhibitors with potent anti-proliferative activity, J Mol Biol 429 (2017) 2211–2230, https://doi.org/10.22034/chemm.2021.130448.
[46] B. Wang, H. Wu, C. Hu, H. Wang, J. Liu, W. Wang, Q. Liu, An overview of kinase downregulators and recent advances in discovery approaches, Signal Transduct Targeted Ther 6 (2021) 423, https://doi.org/10.1038/s41392-021-00826-7.
[47] N. Ashraf, A. Asari, N. Yousaf, M. Ahmad, M. Ahmed, A. Faisal, M. Saleem, M. Muddassar, Combined 3D-QSAR, molecular docking and dynamics simulations studies to model and design TTK inhibitors, Front Chem 10 (2022) 1003816, https://doi.org/10.3389/fchem.2022.1003816.
[48] L. Xing, J. Klug-Mcleod, B. Rai, E.A. Lunney, Kinase hinge binding scaffolds and their hydrogen bond patterns, Bioorg Med Chem 23 (2015) 6520–6527, https://doi.org/10.1016/j.bmc.2015.08.006.